Iranian Journal of Oil & Gas Science and Technology, Vol. 3 (2014), No. 1, pp. 54-64
http://ijogst.put.ac.ir

Resonance Ultrasonic Spectroscopy of a Nanofibrous Composite and Studying the Effect of Surface/Interface

Kobra Kalvandi and Sina Sodagar*

Department of Technical Inspection Engineering, Petroleum University of Technology, Abadan, Iran

Received: September 19, 2013; *revised:* November 16, 2013; *accepted:* December 21, 2013

Abstract

Resonances are intrinsic characteristics of an elastic object, which are completely independent of the source of excitation. The appropriate utilization of the information contained within the resonance spectra and the identification of the resonance frequencies of the object can be used as a potent tool for material characterization. In this paper, a new mathematical model for the wave diffraction from a cylindrical nanofiber encased in an elastic matrix is introduced. The new model is used to evaluate the scattered pressure field resulting from normal insonification on a single nanofibrous composite. It is shown that there are specific resonances, which arise from the surface/interface energy between the nanofiber and solid matrix. They can be used to determine the characteristics and properties of fibrous nanocomposites.

Keywords: Diffraction, Resonance Ultrasonic Spectroscopy, Surface/Interface Effect

1. Introduction

In the past decade, ultrasonic wave propagation in composite materials has attracted great interest particularly in the area of nondestructive evaluation. With the rapid development of nanoscience and nanotechnology, there are increasing demands to fabricate nanostructured and nanocomposite materials; this needs to understand the mechanical behavior of nanosized materials which distinctly differs from their macroscopic counterparts. Resonance scattering theory (RST), developed in 1978 by Uberall and coworkers, has presented a tool known as resonance ultrasonic spectroscopy (RUS) for analyzing scattering problems to evaluate ultrasonic and mechanical behaviors of materials (Veksler et al., 1998). For many years, RUS and other acoustic scattering techniques have been used for the remote classification of submerged targets. In recent decades, this technique has also been utilized for material characterization and nondestructive evaluation (NDE) purposes. RUS technique measures the frequencies of the specimen elastic resonances. These frequencies reflect the size, shape, and elastic composition of the sample; each corresponds to a particular bundle of bouncing, interconverting, traveling waves which are exactly repeated at intervals of $1/f$, where f is the resonance frequency. Given a sufficient dataset of observed resonance frequencies, one can make useful inferences about the sample properties.

RST has been applied to various problems including the acoustic wave scattering from fiber-reinforced composites (Doolittle et al., 1968; Flax et al., 1981; Uberal, 1992). Together with the

* Corresponding Author:
Email: sodagar@put.ac.ir

theoretical developments of RST and RUS, the experimental aspects of these processes have also been considered by many researchers. Maze et al. (1981) presented the first experimental quasi-line spectrum obtained by the method of isolation and identification of resonances (MIIR). MIIR provides experimental verification and illustration of RST. Based on MIIR method, Sodagar et al. (2011) presented an optimized alternative approach to obtaining the experimental form function of cylindrical structures in single and multiple scattering problems.

Owing to the increasing ratio of surface/interface area to volume, surface/interface energy has a significant effect on the mechanical behavior of nanostructures such as the overall elastic properties of nanosized elements and nanocomposites. Gurtin et al. (1998) developed a surface elasticity model considering the effect of surface or interface. In 2003, the elastic deformation of a nanoinhomogeneity including surface effects was analyzed (Sharma et al., 2003). Dingrevilla et al. addressed the surface effects on the elastic behavior of nanosized elements (Dingrevilla et al., 2005). By using the Papkovitch-Neuber displacement potentials, He and Li (He et al., 2006) evaluated the stress concentration around a nanosized spherical void subjected to a unidirectional remote loading. Chen et al. used the generalized Laplace-Young equation of curved surface in nanosized solids (Chen et al., 2006). Tian and Rajapakse (Tian et al., 2007) used a complex potential method to evaluate the elastic field of an elliptical inhomogeneity including surface effects. Most previous studies on elastic wave problems adopted the classical continuum mechanics theory and did not account for the effects of surface/interface on nanoscales. Most recently, Wang et al. (Wang et al., 2006) and Wang (Wang, 2007) investigated the diffraction of plane compressional wave (P-wave) by a nanosized cavity based on surface elasticity, which displays the significant influences of surface effects on diffraction phenomena. Ru et al. (Ru et al., 2009) used a computational modeling to study the effect of surface/interface on the dynamic stress concentration around a cylindrical nanoinclusion. In the current paper, a mathematical model is developed for the resonance scattering of elastic wave from a cylindrical nanofiber insonified by a plane compressional wave. Moreover, the variation of the compressional and shear diffracted far fields from a nanoinclusion at the normal angle of compressional incident wave including surface/interface energy is studied.

2. Mathematical formulation

In the surface elasticity theory, a surface is regarded as a negligibly thin membrane adhered to the bulk without slipping. The equilibrium and constitutive equations in the bulk of the solid are the same as those in the classical theory of elasticity, but the presence of surface stress gives rise to a non-classical boundary condition. In the bulk of a solid, the equilibrium and constitutive equations are the same as those in the classical theory (Duan et al., 2008):

$$\sigma_{ij,j} = \rho \frac{\partial^2 u_i}{\partial t^2} \tag{1}$$

$$\sigma_{ij} = 2\mu(\varepsilon_{ij} + \frac{\nu}{1-2\nu}\varepsilon_{kk}\delta_{ij}) \tag{2}$$

where, ρ is the mass density of the material; t represents the time; μ and ν stand for shear modulus and Poisson's ratio respectively. σ_{ij} and ε_{ij} are stress and strain tensors in the bulk material respectively. Also, the strain tensor is related to the displacement vector u_i as follows:

$$\varepsilon_{ij} = \frac{1}{2}(u_{i,j} + u_{j,i}) \tag{3}$$

The equilibrium equations on the surface/interface can be expressed as (Duan et al., 2008):

$$f_\alpha + \sigma^s_{\beta\alpha,\beta} = 0 \tag{4}$$

$$< \sigma_{ij} > n_i n_j = \sigma^s_{\alpha\beta} \kappa_{\alpha\beta} \tag{5}$$

where, f_α is the tangential component of the traction in the x_α-direction; n_i is the normal vector of the surface/interface; $\kappa_{\alpha\beta}$ is the curvature of the surface/interface and $< \sigma_{ij} >$ is the jump of bulk stress tensor across the surface/interface. For an isotropic surface/interface, the surface/interface stresses are related to the surface strains as reads:

$$\sigma^s_{\alpha\beta} = 2\mu^s \delta_{\alpha\gamma} \varepsilon_{\gamma\beta} + \lambda^s \varepsilon_{\gamma\gamma} \delta_{\alpha\beta} \tag{6}$$

where, μ^s and λ^s are the elastic properties of the isotropic surface.

2.1. Diffraction of elastic waves by a cylindrical nanoinclusion

A plane ultrasonic wave traveling through an infinite, isotropic medium, incident to an encased infinite isotropic cylindrical nanofiber of radius $r = a$ is considered (Figure 1). The elastic constants and the density of the isotropic medium are respectively denoted by λ_1, μ_1, and ρ_1 and those of the fiber are given respectively given by λ_2, μ_2, and ρ_2. A cylindrical coordinate system (r, θ, z) is chosen so that the *z*-direction coincides with the axis of the cylindrical fiber. The displacement field $\vec{u}(r, \theta, z, t)$ in both the matrix and cylinder can be expressed in terms of three scalar potentials, namely φ, χ and ψ (Honarvar et al., 1996):

$$\vec{u} = \nabla\varphi + \nabla \times (\chi \hat{e}_z) + a.\Delta \times \Delta \times (\psi e_z) \tag{7}$$

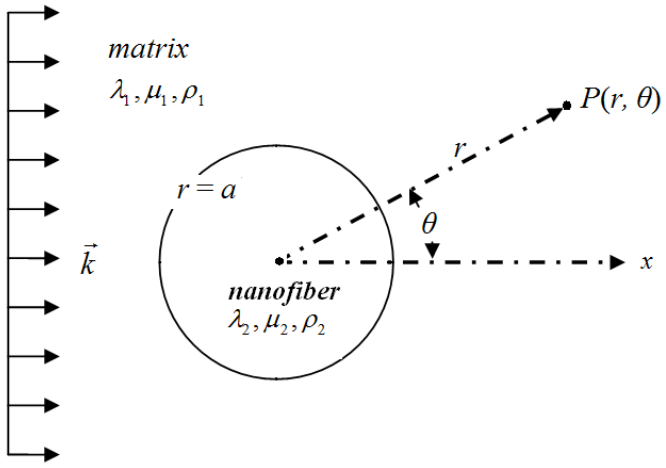

Figure 1
Insonification of acoustic wave to a nanocylindrical inclusion.

At normal wave incident, using Morse-Feschbach decomposition for two dimensional wave problems, the displacement field $\vec{u}(r, \theta, t)$ in the matrix medium can be expressed in terms of two scalar potential functions, namely φ and χ as follows (Sodagar et al., 2010):

$$\vec{u} = \nabla\varphi + \nabla \times (\chi \hat{e}_z) \tag{8}$$

For the case where the incident wave is compressional with circular frequency, the associated normalized potential function in the matrix has the general form of (Beattie et al., 1993):

$$\varphi_{1,incident} = \sum_{n=0}^{\infty} \varepsilon_n i^n J_n(k_{P1} r) \cos n\theta \exp(-i\omega t) \tag{9}$$

where, $k_{P1}=\omega/c_p^{(1)}$ is the compressional wave number and $c_p^{(1)}=\sqrt{2\mu_1(1+\nu_1)(1-2\nu_1)^{-1}\rho_1^{-1}}$ stands for the velocity of compressional wave in the matrix medium. The symbol ε_n, the Neumann factor, is defined as:

$$\varepsilon_n=\begin{cases}1 & for\ \ n=0\\ 2 & for\ \ n>0\end{cases}$$

For the shear wave polarized in the $r-\theta$ plane, the associated normalized potential is obtained from:

$$\chi_{1,incident}=\sum_{n=0}^{\infty}\varepsilon_n\, i^n\, J_n(k_{S1}r)\sin n\theta\exp(-i\,\omega t) \tag{10}$$

where, $k_{S1}=\omega/c_s^{(1)}$ is the shear wave number and $c_s^{(1)}=\sqrt{\mu_1/\rho_1}$ represents the velocity of shear wave in the matrix medium. If one considers the component of the displacement field $\vec{u}$ in the matrix material originating from waves diffracted by the cylindrical inclusion, the associated potential functions are given by:

$$\varphi_{1,diffracted}=\sum_{n=0}^{\infty}\varepsilon_n\, i^n\, A_n\, H_n(k_{P1}r)\cos n\theta\exp(-i\,\omega t) \tag{11}$$

$$\chi_{1,diffracted}=\sum_{n=0}^{\infty}\varepsilon_n\, i^n\, B_n\, H_n(k_{S1}r)\sin n\theta\exp(-i\,\omega t) \tag{12}$$

where, H_n represents the Hankel function of the first kind. Making the appropriate substitution from Equations9-12 into Equation 8, the total displacement in matrix medium can now be obtained by summing the incident and diffracted components:,

$$u_1=u_{1,incidnet}+u_{1,diffracted} \tag{13}$$

For the isotropic cylindrical nanofiber, designated by subscript 2, the potential functions should be of the following form (Fan et al., 1999):

$$\varphi_{2,refracted}=\sum_{n=0}^{\infty}C_n\, J_n(k_{p2}r)\cos n\theta\exp(-i\,\omega t) \tag{14}$$

$$\chi_{2,refracted}=\sum_{n=0}^{\infty}D_n\, J_n(k_{s2}r)\sin n\theta\exp(-i\,\omega t) \tag{15}$$

where, $k_{p2}=\omega/c_p^{(2)}$ is the compressional wave number $c_p^{(2)}=\sqrt{2\mu_2(1-\nu_2)(1-2\nu_2)^{-1}\rho_2^{-1}}$ represents the velocity of compressional wave; $k_{S2}=\omega/c_s^{(2)}$ stands for the shear wave number and $c_s^{(2)}=\sqrt{\mu_2/\rho_2}$ denotes the velocity of shear wave in nanofiber media. The strain-displacement relations in cylindrical coordinate system can be expressed as:

$$\varepsilon_{rr}=\frac{\partial u_r}{\partial r} \tag{16}$$

$$\varepsilon_{\theta\theta}=\frac{1}{r}\frac{\partial u_\theta}{\partial\theta}+\frac{u_r}{r} \tag{17}$$

$$\varepsilon_{r\theta}=\frac{1}{2}\left(\frac{1}{r}\frac{\partial u_r}{\partial\theta}+\frac{\partial u_\theta}{\partial r}-\frac{u_\theta}{r}\right) \tag{18}$$

The constitutive relations from Equation 2 can be rewritten as:

$$\sigma_{rr}=2\mu\left(\varepsilon_{rr}+\frac{\nu}{1-2\nu}(\varepsilon_{rr}+\varepsilon_{\theta\theta})\right) \tag{19}$$

$$\sigma_{\theta\theta}=2\mu\left(\varepsilon_{\theta\theta}+\frac{\nu}{1-2\nu}(\varepsilon_{rr}+\varepsilon_{\theta\theta})\right) \tag{20}$$

$$\sigma_{r\theta} = 2\mu\varepsilon_{r\theta} \tag{21}$$

Therefore, the stress components can be obtained by the substitution of Equation 8 into Equations 16-18 and Equations 1921 respectively.

2.2. Boundary conditions

For an encased infinite fiber, the plane strain assumption $(\varepsilon_{zz} = 0)$ can be used. For the considered plane strain problem, the strain component $\varepsilon^s_{\theta\theta}$ is given by:

$$\varepsilon^s_{\theta\theta} = \frac{1}{2\mu_1}[(1-\nu_1)\sigma_{\theta\theta} - \nu_1\sigma_{rr}]. \tag{22}$$

The interface stress $\sigma^s_{\theta\theta}$ between fiber and matrix can be obtained from Equation 6 as reads:

$$\sigma^s_{\theta\theta} = (2\mu^s + \lambda^s)\varepsilon^s_{\theta\theta} \tag{23}$$

Also, at the fiber/matrix interface $(r = a)$ the continuity of displacements implies that:

$$u_{r1} = u_{r2} \tag{24}$$

$$u_{\theta 1} = u_{\theta 2} \tag{25}$$

In the presence of interface effects, the equilibrium equation can be expressed as:

$$\sigma_{rr1} - \sigma_{rr2} = \frac{\sigma^s_{\theta\theta}}{a} \tag{26}$$

$$\sigma_{r\theta 1} - \sigma_{r\theta 2} = -\frac{1}{a}\frac{\partial\sigma^s_{\theta\theta}}{\partial\theta} \tag{27}$$

By substituting Equations 22 and 23 into Equations 26 and 27, one may obtain:

$$\sigma_{rr1} - \sigma_{rr2} = s[(1-\nu_1)\sigma_{\theta\theta 1} - \nu_1\sigma_{rr1}] \tag{28}$$

$$\sigma_{r\theta 1} - \sigma_{r\theta 2} = -s(1-\nu_1)\frac{\partial\sigma_{\theta\theta}}{\partial\theta} + s\nu_1\frac{\partial\sigma_{rr1}}{\partial\theta} \tag{29}$$

where, $s = \dfrac{2\mu^s + \lambda^s}{2\mu_1 a}$ is a dimensionless parameter reflecting the significance of surface/interface effects. Inserting the displacement components from Equations 8 and 13 and the potential functions from Equations 9-12, 14, and 15 in Equations 24, 27, and 28 results in the following system of four linear algebraic equations:

$$[D_n]\{T_n\} = \{Q_n\} \tag{30}$$

where,

$$\{T_n\} = [A_n \quad B_n \quad C_n \quad D_n]^T \tag{31}$$

$$\{Q_n\} = [b_1 \quad b_2 \quad b_3 \quad b_4]^T \tag{32}$$

$[D_n]$ is 4×4 matrix with components designated as a_{ij}. Equation 30 can be solved for unknown coefficients at any given value of normalized frequency *ka*. For the case of incident compression waves, the resulting normalized resonance spectrum can be obtained as follows (Rhee et al., 1996):

$$f(\theta, Kp_1a) = \sum_{n=0}^{n=\infty}\left(\frac{2}{i\,\pi Kp_1a}\right)(-1)^n\varepsilon_n\frac{(Q_n - Q_n^r)}{(1+2Q_n^r)} \tag{33}$$

For the case of incident shear waves, the normalized resonance spectrum is obtained from:

$$f(\theta, Ks_1a) = \sum_{n=0}^{n=\infty}\left(\frac{2}{i\,\pi Ks_1a}\right)(-1)^n\varepsilon_n\frac{(Q_n - Q_n^r)}{(1+2Q_n^r)} \tag{34}$$

The parameter Q_n, which is equal to one of the coefficients A_n and B_n, depends on the type of the diffracted wave and Q_n^r depends on the type of incident wave as reads:

$$Q_n^r = -\frac{J_n^{'}(Kp_1a)}{H_n^{(1)'}(Kp_1a)} \text{ for incident compression waves} \tag{35}$$

$$Q_n^r = -\frac{J_n^{'}(Ks_1a)}{H_n^{(1)'}(Ks_1a)} \text{ for incident shear waves} \tag{36}$$

3. Numerical results

To examine the validity of the proposed mathematical formulation, the diffracted field of an alumina cylindrical nanoinclusion embedded in an isotropic aluminum matrix is calculated for normal incident angle within the frequency range of $0 < ka < 10$. The verification of the proposed model is accomplished by considering the surface/interface effect as s=0. The far-field backscattered spectrum of the diffracted wave from an alumina cylindrical nanoinclusion with a radius of 2 nm has been calculated and plotted in Figure 2. The resultant form function shows good agreement with the classical solution of a cylindrical inclusion embedded in an isotropic matrix without a surface/interface effect as given elsewhere (Sodagar et al., 2006).

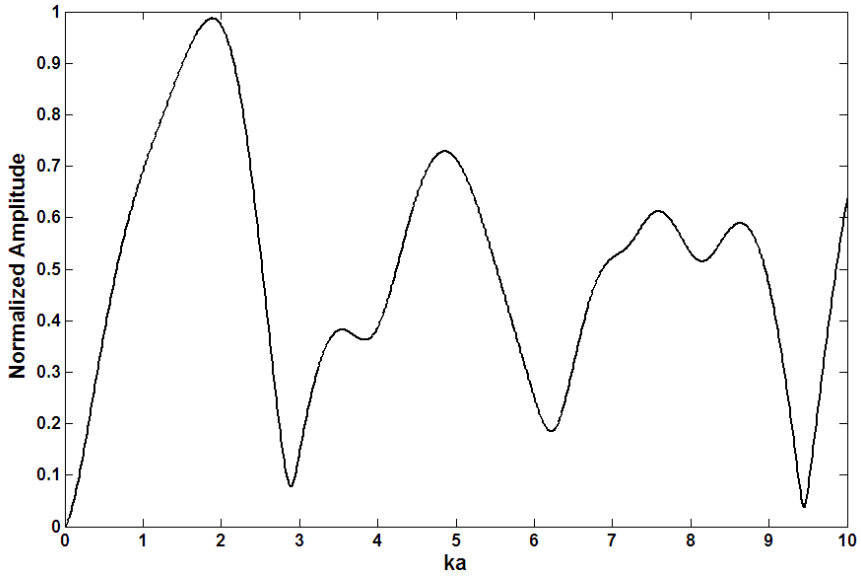

Figure 2
Compressional wave form function of an aluminum/alumina composite material at normal incident angle of compressional wave without an interfacial effect (s = 0).

In order to study the effect of surface/interface energy (interfacial effect) on the diffracted wave, the following set of analysis was performed. A normally incident compressional plane wave illuminates a copper nanofiber embedded in an aluminum matrix. The elastic properties of the materials are given in Table 1. The far-field backscattered resonance spectra and the corresponding phase spectra are calculated without considering the surface/interface effect, i.e. s=0, and including the surface/interface effect, i.e. s=90 (Figures 3a and 3b).

Comparing the resonance spectrum at s=0 (Figure 3a) with the resonance spectrum at s = 90 as shown in Figure 3b shows that including the surface/interface effect into the boundary between the nanofiber and matrix results in appearing new resonance frequencies in the resonance frequency spectrum. It

also shows that there are specific resonances in the wave scattering from a nanosized cylindrical fiber embedded in a solid matrix, which arises from the surface/interface energy between the nanofiber and solid matrix. This means that these resonances can be used to determine the nanocharacteristics and properties of the nanocomposite materials. Figures 4a and 4b show the far-field backscattered resonance spectrum and phase diagram of a copper nanofiber/aluminum matrix for a dipole mode (n=1) for s=0 and s=90; the results confirm the presence of specific resonances arising from the surface/interface energy.

(a)

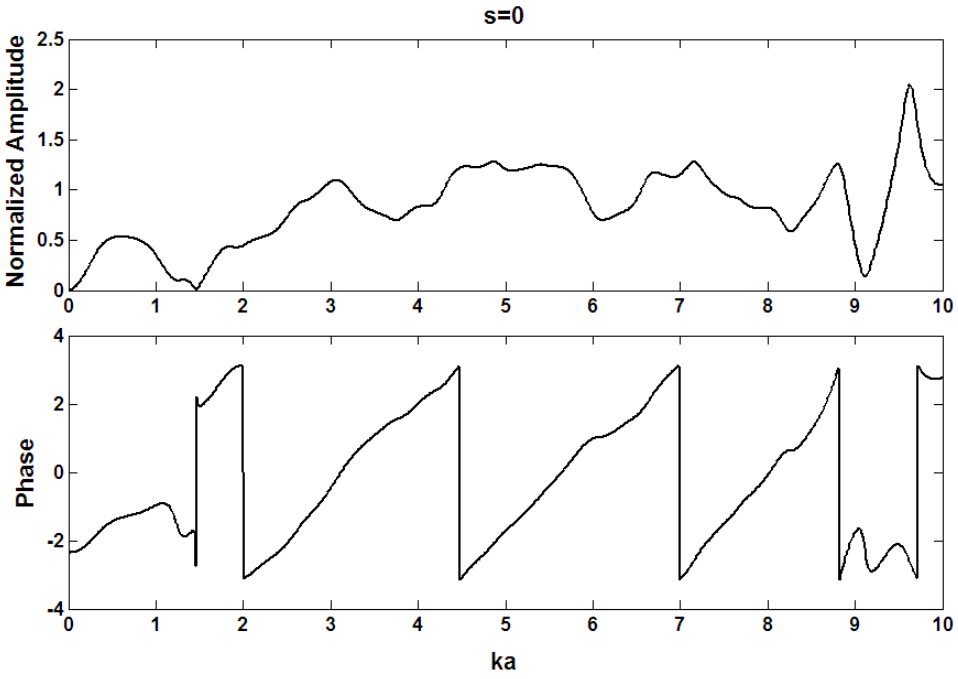

(b)

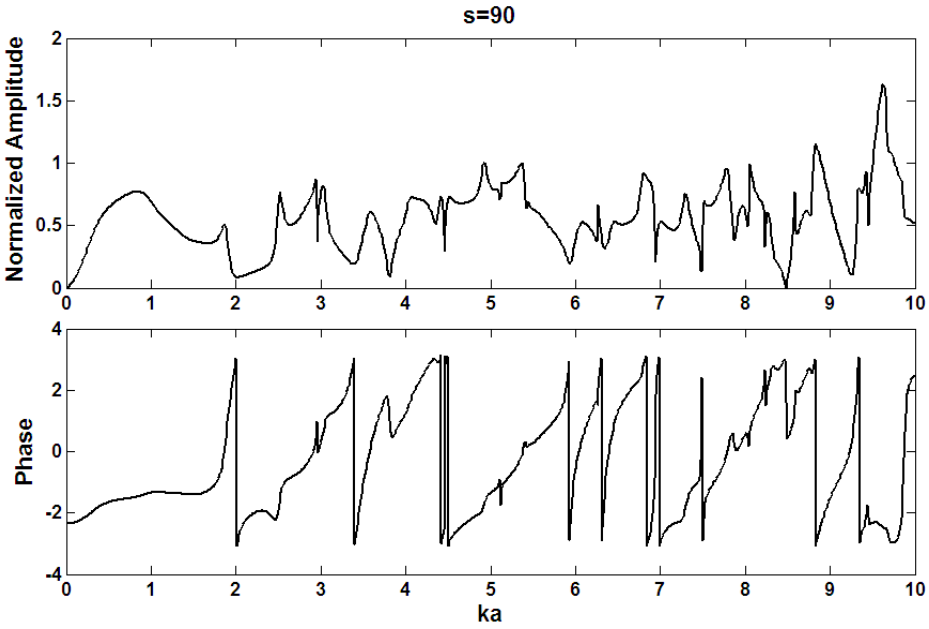

Figure 3
The far-field backscattered resonance and phase spectrum of a copper nanofiber/aluminum matrix for a: s=0 and b: s=90.

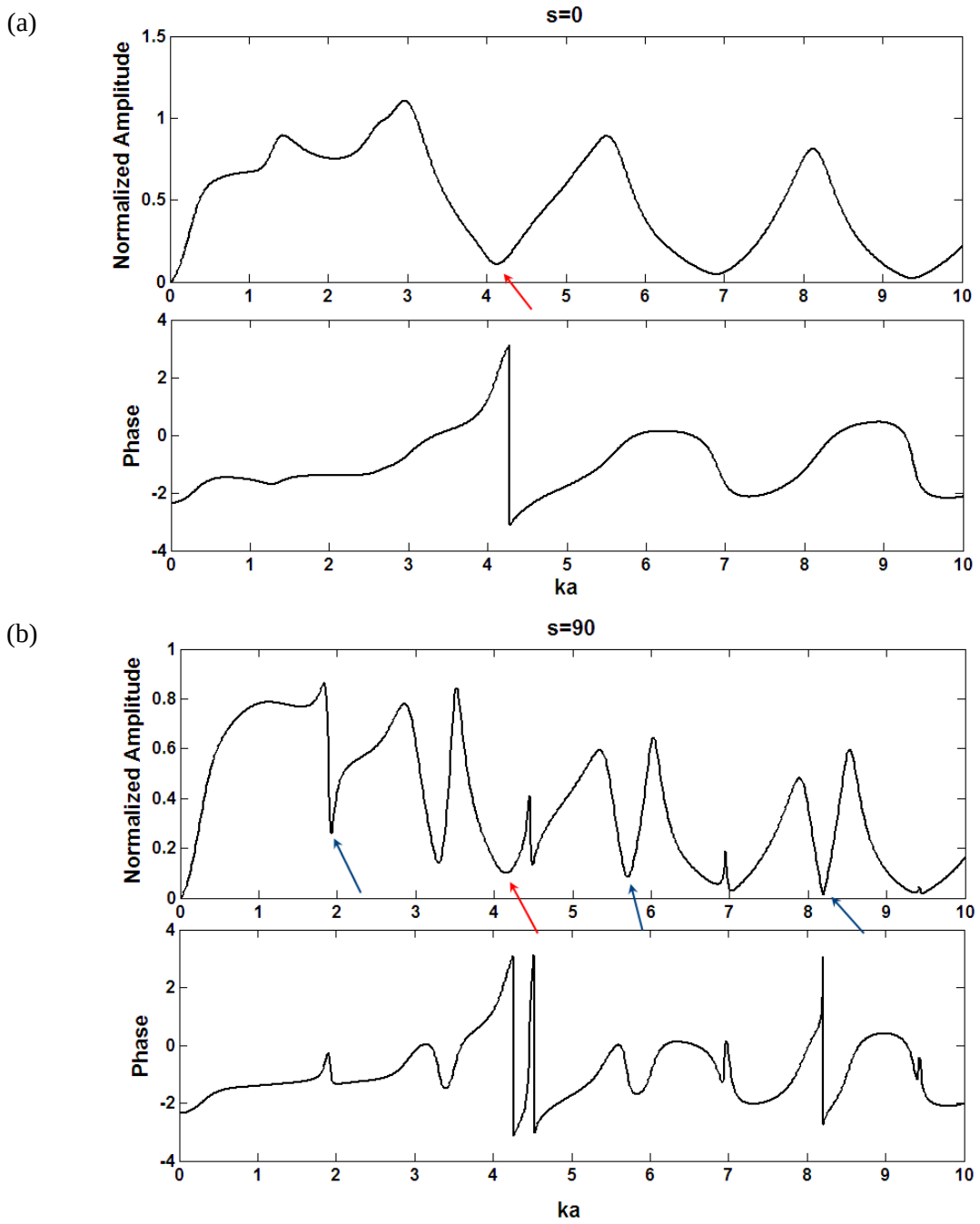

Figure 4
The far-field backscattered resonance spectrum and phase diagram of a copper nanofiber/aluminum matrix for n=1 (the red signs show resonances at s=0 and the blue signs show new resonances); a: s=0 and b: s=90.

In order to study the effect of the surface/interface parameter between the nanofiber and medium, the variation of the far-field backscattered resonance spectra of a copper nanofiber/aluminum matrix with considering changes in surface/interface effect was calculated. The corresponding resonance spectrum for a dipole mode and the form function are shown in Figures 5 and 6 respectively. It can be seen that by increasing the surface/interface energy, the new resonances corresponding to the nanosized characteristics shift to the higher frequencies; finally, beyond a critical interfacial parameter, the surface/interface does not affect the resonances and the frequency of new resonances remains

constant.

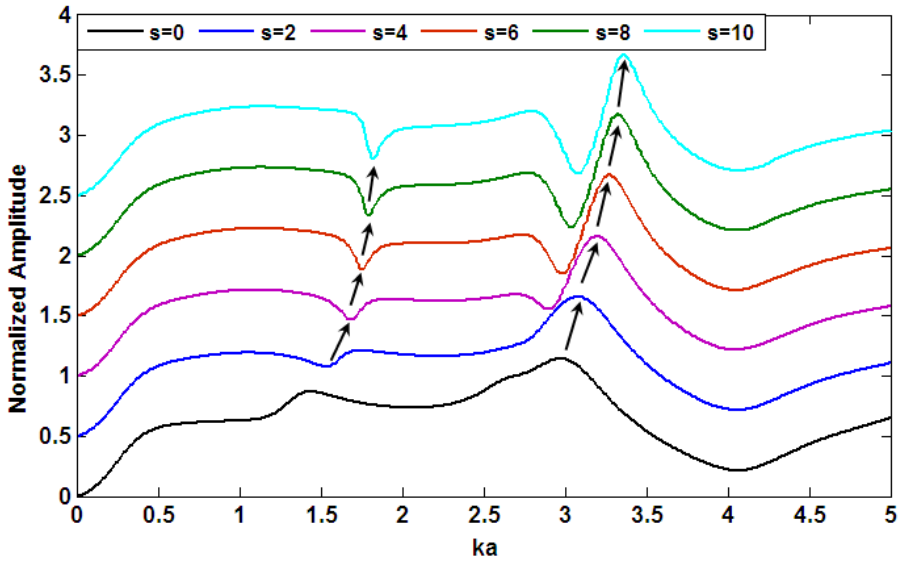

Figure 5
Variation of the far-field backscattered resonance spectra of a copper nanofiber/aluminum matrix for *n*=1 with considering changes in surface/interface effect.

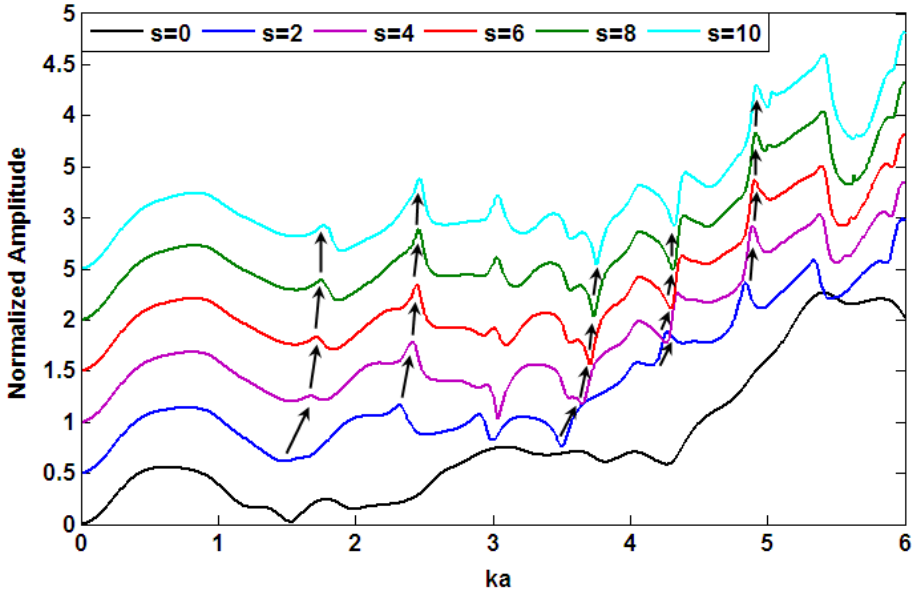

Figure 6
Variation of the far-field backscattered spectrum, form function, of a copper nanofiber/aluminum matrix with considering changes in surface/interface effect.

Table 1
Elastic properties of the materials.

	Density (kg/m^3)	Lame constant, λ, (GPa)	Lame constant, μ, (GPa)
Aluminum	2600	41	25
Copper	8933	15.7	48.3

5. Conclusions

In the current paper, a new mathematical model for the wave diffraction from a cylindrical nanofiber encased in an elastic matrix was introduced. This new model can be used for evaluating the scattered pressure field resulting from the normal insonification of ultrasonic wave in a single nanofibrous composite. The comparison of the numerical results with the previous works confirms the validity of the model. It was also shown that there were specific resonances arising from the surface/interface energy between the nanofibers and the solid matrix; therefore, they can be used to determine the nanocharacteristics and properties of the nanocomposite materials. Moreover, it was shown that by increasing the surface/interface effect the new resonances corresponding to the nanosized characteristics shifted to higher frequencies.

Nomenclature

C_s	: Velocity of shear wave
C_p	: Velocity of compressional wave
H_n	: Hankel function of the first kind
J_n	: Bessel function of the first kind of order n
k_p	: Compressional wave number
k_s	: Shear wave number
RST	: Resonance scattering theory
RUS	: Resonance ultrasonic spectroscopy
s	: Surface/interface parameter
t	: Time
ε_n	: Neumann factor
μ and λ	: Elastic constants
ψ, ϕ, and χ	: Scalar potentials
ν	: Poisson's ratio
ρ	: Mass density
ω	: Circular frequency

Reference

Beattie, P. Chivers., R. C., and Anson, L. W., Ultrasonic Backscattering from Solid Cylindrical Inclusions in Solid Elastic Matrices: A Comparison of Theory and Experiment, J. Acoust. Soc. Am., Vol. 94, No. 6, p.3421-3427, 1993.

Chen, T. Y., Chiu, M. S. and Weng, C. N., Derivation of the Generalized Young-Laplace Equation of Curved Interfaces in Nanoscaled Solids, J. Appl. Phys., Vol. 100, p. 74308 (1-5), 2006.

Dingrevilla, R., Qu., J., and Cherkaoui, M., Surface Free Energy and its Effect on the Elastic Behavior of Nanosized Particles, Wires and Films, J. Mech. Phys. Solids, Vol. 53, p. 1827-1854, 2005.

Doolittle, R. D., Uberall H., and Ugincuis, P., Sound Scattering by Elastic Cylinders, J. Acoust. Soc. Am., Vol. 43, No. 1, p. 1-14, 1968.

Duan H. L., Wang J., and Karihaloo B. L., Theory of Elasticity at Nanoscale, Advances in Applied Mechanics, Vol. 42, p. 30-47, 2008.

Flax, L., Gaunaurd, G. C., and Uberall, H., Theory of Resonance Scattering, in Physical Acoustics, W. P. Mason and R. N. Thurston, Eds., Academic, New York, Vol. 15, p. 191, 1981.

Fan, Y., Sinclair, A. N., and Honarvar, F., Scattering of a Plane Acoustic Wave from a Transversely Isotropic Cylinder Encased in a Solid Elastic Medium, J. Acoust. Soc. Am., Vol. 106, No. 3, p. 1229-1236, 1999.

Gurtin, M. E., Weissmuller, J., and Larche, F., A General Theory of Curved Deformable Interfaces in Solids at Equilibrium, Philos. Mag., Vol. A78, p. 1093-1109, 1998.

He, L. H., and Li, Z. R., Impact of Surface Stress on Stress Concentration, Int. J. Solids and Struct., Vol. 43, p. 6208-6219, 2006.

Honarvar, F. and Sinclair, A. N., Acoustic Wave Scattering from Transversely Isotropic Cylinders, J. Acoust. Soc. Am., Vol. 100, p. 57-63, 1996.

Kim, J. Y. and Ih, J. G., Scattering of Plane Acoustic Waves by a Transversely Isotropic Cylindrical Shell-Application to Material Characterization, Applied Acoustics, Vol. 64, p. 1187-1204, 2003.

Maze, G., Taconet, B., and Ripoche, J., Influence des Ondes de Galerie à Echo sur la Diffusion D'une onde Ultrasonore Plane Par un Cylindre, Phys. Lett. A, Vol. 84, p. 309-312, 1981.

Rhee, H. and park, Y., Novel Acoustic Wave Resonance Scattering Formalism, J. Acoust. Soc., Am., Vol. 102, p. 3401-3412, 1997.

Ru, Y., Wang, G. F., and Wang, T. J., Diffraction of Elastic Waves and Stress Concentration near a Cylindrical Nanoinclusion Incorporating Surface Effect, J. Vib. and Acoust., Vol. 131, p. 061011 (1-7), 2009.

Sharma. P., Ganti, S., and Bhate, N., Effect of Surfaces on the Size-dependent Elastic State of Nanoinhomogenities, Appl. Phys. Lett., Vol. 82, p. 535-537, 2003.

Sodagar, S., Honarvar, F., and Sinclair, A. N., Acoustic Wave Scattering from an Encased Clad Rod, The Thirteenth International Congress of Sound and Vibration (ICSV13), Vienna, Austria, July, 2006.

Sodagar, S. and Honarvar, F., Improvements to the Mathematical Model of Acoustic Wave Scattering from Transversely Isotropic, Scientia Iranica, Trans. B, Vol. 17, No. 3, p. 157-166, 2010.

Sodagar, S., Honarvar, F., Yaghootian, A., and Sinclair, A. N., An Alternative Approach for Measuring the Scattered Acoustic Pressure Field of Immersed Single and Multiple Cylinders, Acoustical Physics, Vol. 57, No. 3, p. 411-419, 2011.

Tian, L. and Rajapakse, R. K. N. D, Elastic Field of an Isotropic Matrix with a Nanoscale Elliptical Inhomogeneity, Int. J. Solids and Struct. Vol. 44, p. 7988-8005, 2007.

Uberal, H., Acoustic Resonance Scattering, Gordon and Breach Science Publishers, p. 341, 1992.

Veksler, N., Izbicki, J. L., and Conoir, M. L., Elastic Wave Scattering by a Cylindrical Shell, J. Acoust. Soc. Am., Vol. 29, p. 195-209, 1998.

Wang, G. F., Wang, T. J., and Feng, X. Q., Surface Effects on the Diffraction of Plane Compressional Waves by a Nanosized Circular Hole, Appl. Phys. Lett., Vol. 89, p. 231923 (1-3), 2006.

Wang, G. F., Diffraction of Plane Compressional Wave by a Nanosized Spherical Cavity with Surface Effects, Appl. Phys. Lett.,Vol. 90, p. 211907 (1-3), 2007.